Oscillatory Behavior of the Tunneling Current in Germanium in a Longitudinal Magnetic Field*

W. BERNARD, S. GOLDSTEIN, H. ROTH, AND W. D. STRAUB
NASA/Electronics Research Center, Cambridge, Massachusetts

AND

J. E. MULHERN, JR.
University of New Hampshire, Durham, New Hampshire

(Received 25 September 1967)

A detailed investigation of the effect of longitudinal magnetic fields up to 110 kOe on the reverse current in Sb-doped germanium tunnel diodes has been carried out in the neighborhood of 4.2°K. The application of a high magnetic field gives rise to a previously reported decrease in the direct interband tunneling current. In addition, small oscillations are observed superimposed on the tunneling current as a function of both magnetic field and bias voltage. To delineate more clearly the oscillatory behavior, an experimental arrangement incorporating a differentiating technique has been utilized to provide direct measurement of dI/dH. The data are analyzed in terms of a model based on the formation of collision-broadened Landau levels. The experimental results reflect the detailed magnetic structure of the (000) conduction band, but are such that the analysis is relatively insensitive to the detailed magnetic structure of the light-hole valence band and the particular choice of tunneling selection rules. Using reasonable values of the collision lifetime, the predictions of this model are in good agreement with experiment.

I. INTRODUCTION

In a previous paper[1] we reported on the effect of longitudinal and transverse magnetic fields on direct interband tunneling in germanium tunnel diodes. In both cases a significant decrease in the reverse tunneling current was observed for voltages greater than the Kane voltage V_k, which corresponds to the onset of direct tunneling. For $\mathbf{H}\perp\mathbf{I}$, V_k was found to increase quadratically with magnetic field. A phenomenological treatment based on conventional tunneling theory[2] and on the assumption of a magnetic-field-dependent Kane voltage was developed to account for the experimental observations. Subsequently, a more fundamental theoretical description of the transverse case has been given by Aronov and Pikus,[3] by Lax *et al.*,[4] and by Reine *et al.*[5]

In Ref. 1, we also reported the presence of small oscillations superimposed on the tunneling current as a function of both magnetic field and bias voltage for the case of $\mathbf{H}\|\mathbf{I}$. A theoretical analysis based on the formation of idealized Landau levels accounted for the existence of the observed oscillatory behavior. In the present paper, we report on modifications and refinements in the experimental techniques, which permit a detailed study of these oscillations. In order to examine the implications of the new experimental results, we also present a more extensive theoretical analysis of the magnetotunneling current.

A qualitative understanding of the origin of the oscillatory behavior can be obtained by referring to Fig. 1, which shows schematic energy–versus–wave-vector curves for the (000) and (111) conduction bands on the n side of the junction and the light-hole valence band on the p side. In the presence of a longitudinal magnetic field, magnetic sub-bands are formed in the (000) conduction band and the light-hole valence band. Neglecting Zeeman spin splitting, the total electronic energy of the nth sub-band in the (000) conduction band is given by

$$\epsilon_{nc}=(n_c+\tfrac{1}{2})\hbar\omega_c+\hbar^2k_{11}^2/2m_c, \qquad (1)$$

where k_{11} is the wave vector parallel to H. The Landau

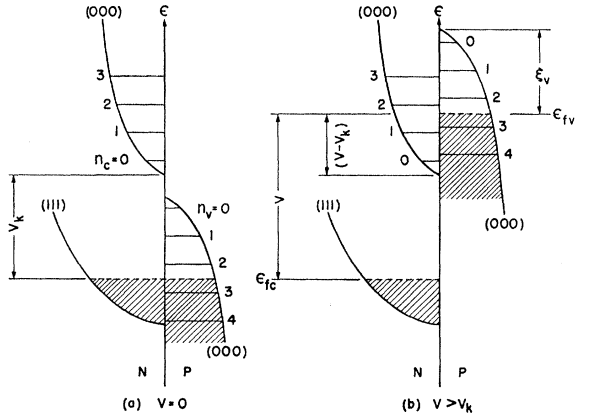

FIG. 1. Schematic energy-level diagram for germanium tunnel junction in the presence of a longitudinal magnetic field, indicating Landau levels in the (000) conduction band on the n side and the light-hole valence band on the p side. The cases of zero bias and a reverse bias $V>V_k$ are shown in parts (a) and (b), respectively.

* Part of this work was performed at the MIT National Magnet Laboratory which is supported by the U. S. Air Force Office of Scientific Research.

[1] H. Roth, W. Bernard, W. D. Straub, and J. E. Mulhern, Jr., Phys. Rev. **145**, 667 (1966).

[2] E. O. Kane, J. Appl. Phys. **32**, 83 (1961).

[3] A. G. Aronov and G. E. Pikus, Zh. Eksperim i Teor. Fiz. **51**, 281 (1966) [English transl.: Soviet Phys.—JETP **24**, 188 (1967)].

[4] B. Lax, M. Weiler, W. Zawadzki, and M. Reine, Bull. Am. Phys. Soc. **12**, 100 (1967).

[5] M. Reine, Q. H. F. Vrehen, and B. Lax, Phys. Rev. (to be published).

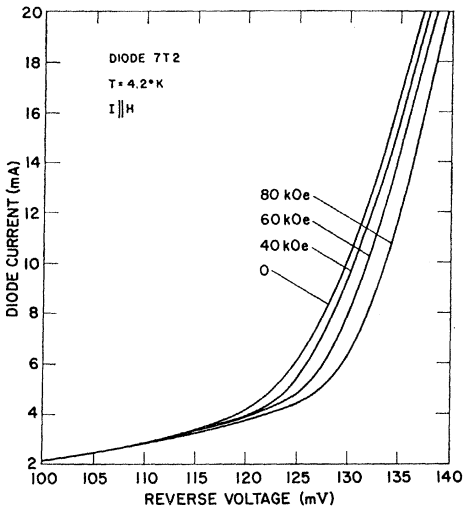

FIG. 2. Current-voltage characteristics for a reverse biased germanium tunnel diode at 4.2°K with longitudinal magnetic field as the parameter.

levels, labeled n_c in the figure, are obtained from Eq. (1) by setting $k_{\parallel}=0$ and represent the lowest allowed electronic energies in the corresponding magnetic sub-bands. Similarly, the Landau levels n_v represent the maximum allowed electronic energies in the magnetic sub-bands of the light-hole valence band. Fig. 1(a) shows the energy diagram of the junction in a magnetic field at zero applied voltage. For a reverse voltage $V>V_k$, direct tunneling can occur between the light-hole valence band and the (000) conduction band. This situation is shown in Fig. 1(b). As the magnetic field is increased at constant V, structure in the tunneling current may arise in three distinct ways: (1) A conduction-band Landau level crosses the valence-band Fermi level ϵ_{fv} before the corresponding valence-band level crosses ϵ_{fv}. (2) A valence-band Landau level crosses ϵ_{fv} before the corresponding conduction-band level crosses ϵ_{fv}. (3) Two corresponding Landau levels in the conduction and valence bands cross each other while they lie below ϵ_{fv}. We note that processes (2) and (3) are incompatible with process (1). As can be seen from Fig. 1, oscillations arising from processes (1) and (3) can also be obtained by varying the bias voltage at constant H. Process (1) reflects the magnetic structure of the (000) conduction band and occurs only at low reverse bias. Assuming that $m_c=m_v$ and that the quantum number n is conserved in tunneling, the low-bias case is defined by $(V-V_k)<\xi_v$. Processes (2) and (3), which occur at high bias, reflect in addition the magnetic structure of the light-hole valence band. Since we have not experimentally observed oscillatory behavior characteristic of processes (2) and (3), we direct ourselves primarily to a discussion of the low-bias case in the present paper.

In Sec. II, we discuss the experimental procedure, including a method for measuring directly dI/dH as a function of V and H. Magnetotunneling oscillations obtained using this differentiating technique are described. In Sec. III, a theoretical analysis of the tunneling process involving collision-broadened Landau levels is presented. Section IV gives a comparison between theory and experiment. Good quantitive agreement is obtained using values of the (000) conduction-band parameters appearing in the literature and realistic collision-broadening lifetimes.

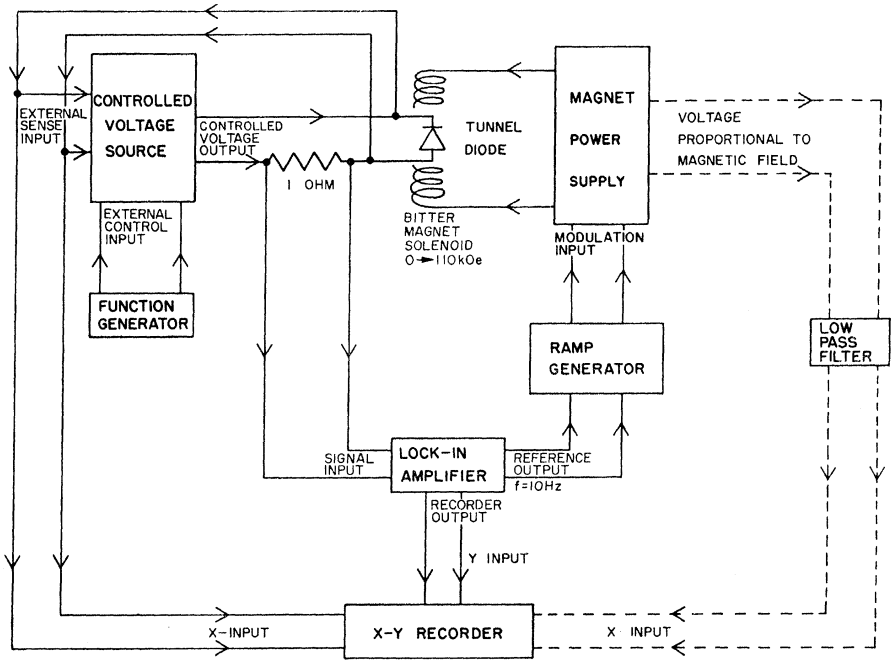

FIG. 3. Block diagram of circuit used in the measurement of dI/dH as a function of bias voltage or magnetic field (dashed circuit).

II. EXPERIMENTAL

Magnetotunneling experiments were carried out in the temperature range from 1.3 to 4.2°K on a number of reverse biased germanium tunnel diodes. The diodes were fabricated with In-Ga-Zn dots alloyed on base material doped to degeneracy with antimony. Such diodes have small indirect current components at low temperatures, where the phonon population is negligible. Arsenic- and phosphorus-doped tunnel diodes, on the other hand, show large indirect current components at low temperatures since these impurities can absorb the crystal momentum required for an indirect transition. Crystalline orientations of the base material were (100) and (111). However, the experimental results exhibited no orientation dependence. The diodes were mounted in nonmagnetic microwave packages modified for low-temperature operation.

The effect on the tunneling current of a longitudinal magnetic field, i.e., a field parallel to the current direction, was investigated using dc field intensities up to 110 kOe. A typical magnetic field-dependent current-voltage characteristic is shown in Fig. 2 and has been described in detail in Ref. 1. In that paper, it was pointed out that small oscillations superimposed on the tunneling current as a function of both magnetic field and bias voltage could be detected. Refinements in the experimental approach have resulted in a clear definition of this phenomenon and have led to a detailed analysis of the oscillatory behavior.

The experimental technique, which yields a direct measurement of the derivative of the current with respect to the magnetic field dI/dH can be understood by referring to Fig. 3. An internally generated 10-Hz voltage signal from a PAR Type HR-8 lock-in amplifier is fed into the magnet power supply as an error signal. This results in a 10-Hz modulation of ~1-kOe peak-to-peak superimposed on the dc magnetic field of the Bitter magnet. The voltage at the diode terminals is sensed and controlled by a PAR Type TC-602CR constant voltage source which can be swept by means of an external function generator. In this way, the diode voltage is controlled to 1 part in 10^5.

The modulated current signal, monitored by a 1-Ω precision resistor, is processed by the lock-in amplifier, whose output voltage is proportional to dI/dH and is plotted on an X-Y recorder as a function of bias voltage with magnetic field as a parameter. Alternatively, the sweep feature of the magnet can be used to obtain dI/dH as a function of magnetic field at constant bias voltage.

Typical results of measurements of dI/dH versus V are shown in Fig. 4 for several magnetic fields. Although the temperature indicated is 4.2°K, identical results were obtained at 1.3°K. The modulating magnetic field has an amplitude of 1200-G peak-to-peak. The most striking feature of Fig. 4 is the prominence of the oscillatory behavior. Other features become immediately apparent: The oscillations are superimposed on a monotonically increasing background; the effective Kane voltage increases with increasing magnetic field as discussed previously[1]; and the peaks are uniformly spaced for each value of magnetic field, with the period increasing linearly with H, which implies that the oscillations are related to the formation of Landau levels.

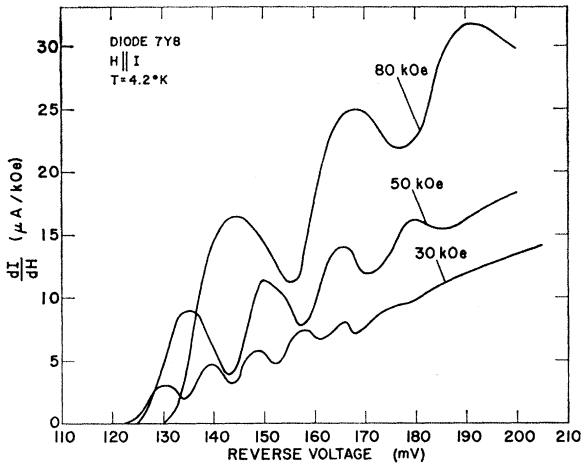

FIG. 4. dI/dH versus reverse bias voltage at 4.2°K for a typical diode with longitudinal magnetic field as the parameter.

It would be expected that Landau levels exist in both the (000) conduction band and the light-hole valence band because of the small effective masses, and that both would contribute to the form taken by the oscillatory behavior. This, together with the possibility of observing spin splitting at higher magnetic fields, makes the regularity and simplicity of the shape of particular interest. It is to be expected that the lack of structure is due in part to collision broadening. The implications of these results are discussed in the following sections.

III. THEORETICAL

We now discuss the calculation of the tunnel current in the presence of a longitudinal magnetic field, introducing those modifications appropriate to the analysis of the present data. In particular, it is necessary to include the effects of collision broadening of the Landau levels in order to achieve detailed agreement with experiment.

According to Kane's theory of direct interband tunneling,[2] the transmission coefficient in the absence of a magnetic field is

$$T=\tfrac{1}{9}\pi^2 \exp(-\pi m^{*1/2}\epsilon_g^{3/2}/2\hbar E) \exp(-\epsilon_\perp/\bar{\epsilon}_\perp), \quad (2)$$

where ϵ_g is the direct band gap, $E=E_0(1+V/V_b)^{1/2}$ is the junction electric field, $m^*=m_c m_v/(m_c+m_v)$ is the reduced tunneling mass for the (000) conduction band of mass m_c and the light-hole valence band of mass m_v, and V_b is the junction built-in voltage. The energy $\epsilon_\perp$

transverse to the direction of current flow is

$$\epsilon_\perp = \hbar^2 k_\perp^2/2m^*, \tag{3}$$

where $k_\perp$ is the transverse wave vector. The quantity $\tilde{\epsilon}_\perp$ appearing in Eq. (2) is given by

$$\tilde{\epsilon}_\perp = e\hbar E/\pi m^{*1/2}\epsilon_g^{1/2}. \tag{4}$$

The application of a longitudinal magnetic field gives rise to cyclotron orbits quantized in a plane transverse to the direction of current flow. For this case, $\epsilon_\perp$ appearing in Eq. (2) is replaced by the sum of the cyclotron energies of each pair of Landau levels between which tunneling occurs. We note that, while the (000) conduction-band minimum appears to exhibit a standard Landau level form, there are indications from optical-absorption studies[6,7] that the magnetic structure of the light-hole valence band may be somewhat more complex. Since the results reported in the present work are rather insensitive to the details of the valence-band structure, however, we adopt a model incorporating standard Landau levels for both bands. In order to include the effect of collision broadening on the tunneling probability, we then express the Landau level energies in the conduction and valence bands, respectively, as

$$\begin{aligned} \epsilon_{nc} &= [n+\tfrac{1}{2}(1\pm G_c)]\hbar\omega_c + \Delta\epsilon_{nc}, \\ \epsilon_{nv} &= [n+\tfrac{1}{2}(1\pm G_v)]\hbar\omega_v + \Delta\epsilon_{nv}, \end{aligned} \tag{5}$$

where

$$G_c = (m_c/2m_0)g_c, \quad G_v = (m_v/2m_0)g_v \tag{6}$$

are the normalized g factors.

The probability distribution of the Landau level broadening $\Delta\epsilon_n$ in Eq. (5) is taken to be of the form[8]

$$P(\Delta\epsilon_n) = (2\pi\sigma^2)^{-1/2}\exp\left[-\frac{(\Delta\epsilon_n)^2}{2\sigma^2}\right] \tag{7}$$

for both the conduction and valence bands. In Eq. (7) the standard deviation $\sigma \sim \hbar/(2\sqrt{2}\tau)$, where τ is a scattering relaxation time representative of both the conduction and valence bands.

The complexities in the true magnetic structure of the light-hole valence band can lead to corresponding complexities in the selection rules for tunneling. However, the insensitivity of our results to the details of the valence-band structure mentioned above makes it reasonable to assume here that the Landau quantum number n is conserved in the tunneling process. Thus, in the magnetic case, the transverse energy $\epsilon_\perp$ appearing in Eqs. (2) and (3) becomes, for the nth Landau level,

$$\epsilon_{n\perp} = [n+\tfrac{1}{2}(1\pm G)]\hbar\omega^* + \Delta\epsilon_{nc} + \Delta\epsilon_{nv}, \tag{8}$$

where

$$G = m^*(G_c/m_c + G_v/m_v) = \tfrac{1}{2}(G_c+G_v) \tag{9}$$

for $m_c = m_v$. Substitution of Eq. (8) into Eq. (2) yields the transmission coefficient for tunneling, in the presence of a longitudinal magnetic field, associated with the nth Landau level as

$$\begin{aligned} T_n^{(\pm)} &= \tfrac{1}{9}\pi^2\exp(-\pi m^{*1/2}\epsilon_g^{3/2}/2e\hbar E) \\ &\times\exp(-\{[n+\tfrac{1}{2}(1\pm G)]\hbar\omega^* + \Delta\epsilon_{nc} + \Delta\epsilon_{nv}\}/\tilde{\epsilon}_\perp), \end{aligned} \tag{10}$$

where the (+) and (−) signs correspond to electrons having corresponding spin directions.

The elementary current incident from the (000) conduction band in the range $d\epsilon_c dk_\perp$ is found to be

$$dI_{\text{inc}}^{(\pm)} = [ae/(2\pi)^2\hbar]d\epsilon_c dk_\perp, \tag{11}$$

where ϵ_c is the total energy of an electron in the conduction band, $k_\perp$ now corresponds to the centers of the harmonic oscillator wave functions along a transverse axis, and a is the area of the junction.

The elementary direct tunneling current dI_n associated with the nth Landau level is obtained by taking the product of Eqs. (7), (10), and (11). Thus,

$$\begin{aligned} dI_n^{(\pm)}(H) = \frac{ae}{36\hbar(2\pi\sigma^2)}\exp\left(-\frac{\pi m^{*1/2}\epsilon_g^{3/2}}{2e\hbar E}\right)\exp\left[-\frac{(\Delta\epsilon_{nc})^2+(\Delta\epsilon_{nv})^2}{2\sigma^2}\right] \\ \times\exp\left\{-\frac{[n+\tfrac{1}{2}(1\pm G)]\hbar\omega^*+\Delta\epsilon_{nc}+\Delta\epsilon_{nv}}{\tilde{\epsilon}_\perp}\right\}d\epsilon_c dk_\perp d(\Delta\epsilon_{nc})d(\Delta\epsilon_{nv}). \end{aligned} \tag{12}$$

The total direct tunneling current is obtained by integrating Eq. (12) over ϵ_c, $k_\perp$, $\Delta\epsilon_{nc}$, and $\Delta\epsilon_{nv}$, and summing over n as

$$\begin{aligned} I^{(\pm)}(H) = \frac{ae}{36\hbar(2\pi\sigma^2)}\exp\left(-\frac{\pi m^{*1/2}\epsilon_g^{3/2}}{2e\hbar E}\right)\sum_n \int_{-\infty}^{(V-V_k)-[n+\frac{1}{2}(1\pm G_c)]\hbar\omega_c} d(\Delta\epsilon_{nc})\int_{-\infty}^{\infty} d(\Delta\epsilon_{nv})\exp\left[-\frac{(\Delta\epsilon_{nc})^2+(\Delta\epsilon_{nv})^2}{2\sigma^2}\right] \\ \times\int_{[n+\frac{1}{2}(1\pm G_c)]\hbar\omega_c+\Delta\epsilon_{nc}}^{(V-V_k)} d\epsilon_c\exp\left\{-\frac{[n+\tfrac{1}{2}(1\pm G)]\hbar\omega^*+\Delta\epsilon_{nc}+\Delta\epsilon_{nv}}{\tilde{\epsilon}_\perp}\right\}\int_{-eH/2\hbar}^{eH/2\hbar} dk_\perp. \end{aligned} \tag{13}$$

The limits appearing in the above expression for $I^{(\pm)}(H)$ can be understood by reference to Fig. 1 and the related discussion in Sec. I. For a given n, the lower limit on ϵ_c is $[n+\frac{1}{2}(1\pm G_c)]\hbar\omega_c+\Delta\epsilon_{nc}$, the lowest allowed conduction-band energy. The corresponding upper limit on ϵ_c is either $(V-V_k)$, the highest occupied level in the valence band,

[6] L. M. Roth, B. Lax, and S. Zwerdling, Phys. Rev. **114**, 90 (1959).
[7] Q. H. F. Vrehen, Phys. Rev. **145**, 675 (1966).
[8] R. B. Dingle, Proc. Roy. Soc. (London) **A211**, 517 (1952). This work shows that the relaxation-time approximation for scattering leads to a Lorenzian broadening of the Landau levels. For reasons of mathematical convenience, however, we have chosen to represent the broadening by a Gaussian probability distribution.

or $(V-V_k+\xi_v)-[n+\frac{1}{2}(1\pm G_v)]\hbar\omega_v+\Delta\epsilon_{nv}$, the highest allowed valence-band energy, whichever is smaller. For the low-bias case, defined by $(V-V_k)<(m_v/m_c)\xi_v$, the appropriate upper limit is $(V-V_k)$ for all values of n contributing appreciably to the tunneling process. Since the oscillations which we have observed experimentally are characteristic only of the low-bias case, we have written the upper limit on ϵ_c in Eq. (13) as $(V-V_k)$. In the low-bias case the valence-band Landau levels which take part in the tunneling process are all assumed to lie above the Fermi level by an energy which is large compared to σ, so that the limits on $\Delta\epsilon_{nv}$ have been taken as $\pm\infty$. However, the integral over $\Delta\epsilon_{nc}$ must have a finite upper limit since only that portion of the level lying below the valence-band Fermi level can contribute to the tunneling. The summation over n in Eq. (13) is carried out from $n=0$ to $n=N$, which corresponds to a conduction-band Landau level lying sufficiently far above the valence-band Fermi level that all higher values of n make a negligible contribution.

Performing the indicated integrations in Eq. (13), we obtain, after some manipulation, the result

$$I^{(\pm)}(H)=\frac{ae\hbar\omega^*}{36\hbar^3}\exp\left(-\frac{\pi m^{*1/2}\epsilon_g^{3/2}}{2e\hbar E}\right)\sum_{n=0}^{N}\left[\left([V-V_k]+\frac{\sigma^2}{\bar{\epsilon}_\perp}-[n+\tfrac{1}{2}(1\pm G_c)]\hbar\omega_c\right)\times\left(\tfrac{1}{2}+\tfrac{1}{2}\,\mathrm{erf}\left\{\frac{[V-V_k]+\sigma^2/\bar{\epsilon}_\perp-[n+\frac{1}{2}(1\pm G_c)]\hbar\omega_c}{(2\sigma^2)^{1/2}}\right\}\right)+\frac{\sigma}{(2\pi)^{1/2}}\exp\left(-\frac{\{[V-V_k]+\sigma^2/\bar{\epsilon}_\perp-[n+\frac{1}{2}(1\pm G_c)]\hbar\omega_c\}^2}{2\sigma^2}\right)\right]\exp\left(\frac{\sigma^2}{\bar{\epsilon}_\perp^2}\right)\exp\left\{-\frac{[n+\frac{1}{2}(1\pm G)]\hbar\omega^*}{\bar{\epsilon}_\perp}\right\}. \quad (14)$$

We note that it is not possible to perform the summation over n explicitly, as in Ref. 1, because of the inclusion of collision broadening.

In order to compare Eq. (14) with experiment, we expand the weak voltage dependence in the tunneling exponent to first order in V and rewrite the expression in the form

$$I^{(\pm)}(H)\simeq\frac{AB}{0.6}\exp(BV)\exp\left(\frac{B^2\sigma^2}{0.09\gamma^2}\right)\sum_{n=0}^{N}\left[\left([V-V_k]+\frac{B\sigma^2}{0.3\gamma}-[n+\tfrac{1}{2}(1\pm G_c)]\hbar\omega_c\right)\times\left(\tfrac{1}{2}+\tfrac{1}{2}\,\mathrm{erf}\left\{\frac{[V-V_k]+B\sigma^2/0.3\gamma-[n+\frac{1}{2}(1\pm G_c)]\hbar\omega_c}{(2\sigma^2)^{1/2}}\right\}\right)+\frac{\sigma}{(2\pi)^{1/2}}\exp\left(-\frac{\{[V-V_k]+B^2\sigma^2/0.3\gamma-[n+\frac{1}{2}(1\pm G_c)]\hbar\omega_c\}^2}{2\sigma^2}\right)\right]\exp\left\{-\frac{B[n+\frac{1}{2}(1\pm G)]\hbar\omega^*}{0.3\gamma}\right\}, \quad (15)$$

where, as in Ref. 1,

$$\gamma=(1+V/V_b)^{1/2} \quad (16)$$

and

$$B=\pi m^{*1/2}\epsilon_g^{3/2}/4e\hbar V_b E_0, \quad (17)$$

E_0 being the zero-bias electric field in the junction. The parameters A, B, and V_k appearing in Eq. (15) are chosen to be consistent with the zero-field tunneling current.

Finally, Eq. (15) can be differentiated with respect to H to yield

$$\frac{dI^{(\pm)}(H)}{dH}=-\frac{ABe\hbar}{0.6m^*}\exp(BV)\exp\left(\frac{B^2\sigma^2}{0.09\gamma^2}\right)\sum_{n=0}^{N}\left[[n+\tfrac{1}{2}(1\pm G_c)]\hbar\omega_c\times\left(\tfrac{1}{2}+\tfrac{1}{2}\,\mathrm{erf}\left\{\frac{[V-V_k]+B\sigma^2/0.3\gamma-[n+\frac{1}{2}(1\pm G_c)]\hbar\omega_c}{(2\sigma^2)^{1/2}}\right\}\right)+\left(1-\frac{B[n+\frac{1}{2}(1\pm G)]\hbar\omega^*}{0.3\gamma}\right)\times\left([n+\tfrac{1}{2}(1\pm G_c)]\hbar\omega_c-[V-V_k]-\frac{B\sigma^2}{0.3\gamma}\right)\times\left(\tfrac{1}{2}+\tfrac{1}{2}\,\mathrm{erf}\left\{\frac{[V-V_k]+B\sigma^2/0.3\gamma-[n+\frac{1}{2}(1\pm G_c)]\hbar\omega_c}{(2\sigma^2)^{1/2}}\right\}\right)-\frac{\sigma}{(2\pi)^{1/2}}\exp\left(-\frac{\{[V-V_k]+B\sigma^2/0.3\gamma-[n+\frac{1}{2}(1\pm G_c)]\hbar\omega_c\}^2}{2\sigma^2}\right)\right]\exp\left\{-\frac{B[n+\frac{1}{2}(1\pm G)]\hbar\omega^*}{0.3\gamma}\right\}. \quad (18)$$

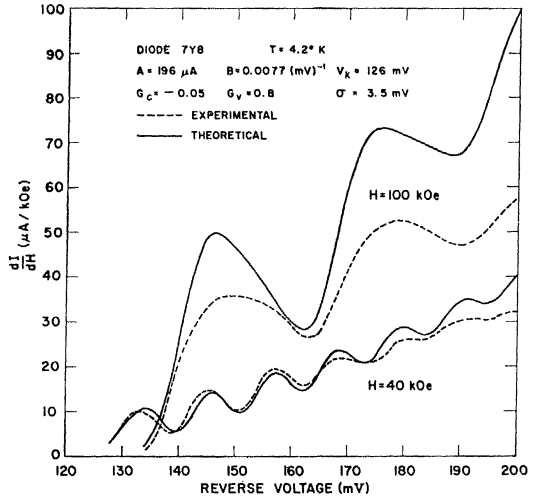

FIG. 5. Comparison between theory and experiment for dI/dH versus V at $H=40$ and 100 kOe.

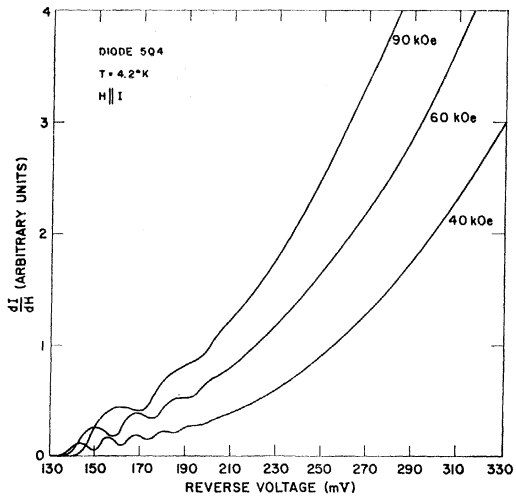

FIG. 7. dI/dH versus reverse bias voltage at 4.2°K for a low-current diode with longitudinal magnetic field as the parameter.

IV. RESULTS AND DISCUSSION

The numerical evaluation of Eq. (18) for dI/dH was carried out using an IBM 360 computer. The parameters A, B, and V_k were chosen to be consistent with the zero-field tunneling characteristic as given by Eq. (7) of Ref. 1,

$$I(0)=A\gamma\exp(BV)\times\left([V-V_k]-\frac{0.15\gamma}{B}\left\{1-\exp\left[-\frac{B(V-V_k)}{0.15\gamma}\right]\right\}\right). \quad (19)$$

Also considered as parameters were the normalized g factors G_c and G_v and the standard deviation σ of the collision broadening.

Figure 5 shows a typical comparison of theory and experiment for dI/dH as a function of V for $H=40$ and 100 kOe. The effective masses in the (000) conduction band and the light-hole valence band were taken to be[9] $m_c=m_v=0.042m_0$, which yields good agreement with the observed period of the oscillations. The theoretical fit was found to be particularly sensitive to the parameters B and σ. The value of σ for this particular diode is 3.5×10^{-3} eV, which corresponds to a relaxation time $\tau\sim7\times10^{-14}$ sec. This agrees with the values of τ obtained from Shubnikov-de Haas experiments on degenerately doped germanium[10] and is of the same order of magnitude as the values obtained from analysis of conductivity measurements.[11] The absence of any fine structure in the oscillations shown in Fig. 5 implies that the Zeeman splitting of the electron spins in the (000) conduction band at $H=100$ kOe is less than the collision broadening, which corresponds to $|g_c|<15$. The value $g_c=-2.5$ ($G_c=-0.05$) used was chosen to correspond to the published estimates.[6,7] Although the results are rather insensitive to the spin splitting in the light-hole valence band, the abnormally large value of $g_v=\pm40$ ($G_v=\pm0.8$) appears to yield the optimum over-all fit to the data. It is possible that this large g factor reflects the more complex magnetic structure of the light-hole valence band as suggested by theoretical considerations and magneto-optical studies.[6,7] It would be expected that discrepancies in the predictions of the simple model would be most pronounced at low quantum numbers, corresponding to high magnetic fields. As is seen in Fig. 5, the agreement between theory and experiment is in fact less satisfactory at the higher field.

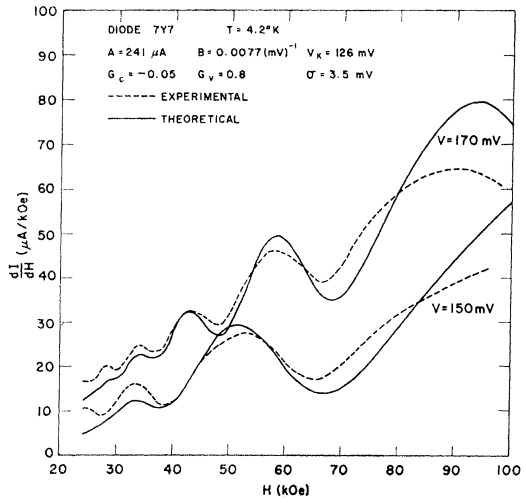

FIG. 6. Comparison between theory and experiment for dI/dH versus H at $V=150$ and 170 mV.

[9] B. Lax, J. G. Mavroides, in *Solid State Physics*, edited by F. Seitz and D. Turnbull (Academic Press Inc., New York, 1960), Vol. 11, p. 390.

[10] W. Bernard, H. Roth, W. D. Straub, and J. E. Mulhern, Jr., Phys. Rev. **135**, A1386 (1964).

[11] W. Bernard, H. Roth, and W. D. Straub, Phys. Rev. **132**, 33 (1963).

The above magnetic band-structure parameters were also used to fit experimental measurements of dI/dH versus H. Typical results are shown in Fig. 6 for reverse bias voltages of 150 and 170 mV.

An attempt was made to observe oscillations of dI/dH in the high-bias region, for which $(V-V_k)>\xi_v$. A low-current diode was used in order to obtain high reverse bias voltages at acceptable power dissipation levels. The results for dI/dH versus V are shown in Fig. 7. According to the discussion in Sec. I in connection with Fig. 1, the period of the oscillations should increase abruptly as the transition is made from the low-bias case [process (1)] to the high-bias case [process (3)]. That no such discontinuous change in period is observed implies either that the high-bias region was never actually attained or that the amplitude of the expected oscillations is below the sensitivity of the instrumentation.

ACKNOWLEDGMENTS

We gratefully acknowledge the hospitality of the MIT National Magnet Laboratory. In particular, we would like to thank L. G. Rubin for his helpful advice on instrumentation. We are also indebted to Dr. A. T. Lewis and Dr. R. C. Williamson of the NASA Electronic Research Center for assistance in writing the programs. Finally, we would like to thank the University of New Hampshire Computation Center for making their facilities available to us.

PHYSICAL REVIEW VOLUME 166, NUMBER 3 15 FEBRUARY 1968

Contribution of Excitons to the Edge Luminescence in Zinc Oxide

R. L. WEIHER AND W. C. TAIT
Central Research Laboratories, 3M Company, Saint Paul, Minnesota
(Received 24 July 1967; revised manuscript received 29 September 1967)

The photoluminescence of "pure" ZnO at 77°K has been investigated. Multiple-emission maxima, both "intrinsic" and "extrinsic," have been observed in the near ultraviolet. Narrow emission bands (half-widths ≤ 3 Å) near 3690 Å are ascribed to the annihilation of bound (impurity) excitons. A broad asymmetrical band (half-width ≈ 22 Å) near 3747 Å is shown to be closely characterized by theory of the annihilation of free (intrinsic) excitons with the simultaneous emission of longitudinal optical phonons. Multiphonon emission bands, separated by approximately the energy of the longitudinal optical phonon, are observed at longer wavelengths. An emission band near 3677 Å is suggested to originate from the "direct" annihilation of free (intrinsic) excitons.

I. INTRODUCTION

THE luminescence of zinc oxide (ZnO) has been the subject of numerous papers.[1–6] The excellent review article on ZnO by Heiland, Mollwo, and Stockmann[1] in 1959 includes a comprehensive summary of the luminescence of ZnO to that data. More recently, several investigations[2–5] have reported on extensive studies of single crystals which have added much to our knowledge on this subject.

The photoluminescence and cathodoluminescence of ZnO near room temperature can be generally characterized by two broad bands, one in the near ultraviolet (uv) and one in the "green" portion of the spectrum. At lower temperatures, both of these broad bands exhibit structure in the form of series of nearly overlapping maxima. The energy separation between adjacent maxima has frequently led investigators to propose that the emission results from the recombination of electron-hole pairs, possibly through exciton states, accompanied by the emission of transverse and/or longitudinal phonons.[1,3] The exact assignment of these maxima, however, has not yet been made. In addition, numerous narrow (line half-widths ≤ 0.1 Å) absorption and emission lines in the near uv have been observed at near liquid-helium temperature.[4,5] These narrow lines have been shown by Reynolds, Litton, and Collins[5] to originate from bound-exciton complexes.

Andress[3] has thoroughly investigated the cathodoluminescence of ZnO crystals near liquid-nitrogen temperature. We refer the reader to that article,[3] or elsewhere,[1,6] for a discussion of the broad-band "green" emission. It was shown by Andress[3] that the near-uv emission at 90°K is nearly plane-polarized with the electric vector perpendicular to the c axis of the wurtzite crystal structure of ZnO. The ratio of intensities for emission polarized parallel and perpendicular to c axis was found experimentally to be

$$I_{\parallel}/I_{\perp}=\exp(-0.035/kT) \quad (1)$$

near 90°K. This observation is consistent with theoret-

[1] G. Heiland, E. Mollwo, and F. Stockmann, in *Solid State Physics*, edited by F. Seitz and D. Turnbull (Academic Press Inc., New York, 1959), Vol. 8.
[2] B. Andress and E. Mollwo, Naturwiss. **46**, 623 (1959).
[3] B. Andress, Z. Physik **170**, 1 (1962).
[4] D. G. Thomas, J. Phys. Chem. Solids **15**, 86 (1960).
[5] D. C. Reynolds, C. W. Litton, and T. C. Collins, Phys. Rev. **140**, A1726 (1965).
[6] P. S. Litvinowa, Zh. Eksperim. i Teor. Fiz. **27**, 636 (1949).